DYNA
http://dyna.medellin.unal.edu.co/

UNIVERSIDAD NACIONAL DE COLOMBIA

A general model for rectangular footings part II: modeling for design

José Benito Rivera-Mendoza, Arnulfo Luévanos-Rojas, Sandra López-Chavarría, Manuel Medina-Elizondo & Marylú García-Galván

Instituto de Investigaciones Multidisciplinarias, Universidad Autónoma de Coahuila, Torreón, Coahuila, México. benitoriveramendoza@hotmail.com, arnulfol_2007@hotmail.com, sandylopez5@hotmail.com, drmanuelmedina@yahoo.com.mx, marylugarciagalvan@live.com.mx

Received: December 10th, 2021. Received in revised form: April 25th, 2022. Accepted: May 4th, 2022.

Abstract
This paper presents a general model for the design to obtain the thickness and reinforcing steel areas of rectangular footings that support from 1 to "*n*" columns aligned on a longitudinal axis. The pressure diagram is considered linear. Some recently published papers are restricted to certain types of footings as the rectangular isolated footings, and rectangular combined footings that support two columns. The first part of this paper shows the minimum soil area that supports 1 to "*n*" columns aligned on a longitudinal axis. Three numerical examples are presented for design of rectangular footings subjected to an axial load and two orthogonal moments in each column that supports one, two and three columns. The main advantage of this document over other documents is: this model can be applied for one or more columns supported on a rectangular footing (unrestricted on its sides, one side restricted and two opposite sides restricted).

Keywords: general model for rectangular footings; modeling for design; rectangular isolated footings; rectangular combined footings.

Un modelo general para zapatas rectangulares parte II: modelado para diseño

Resumen
Este artículo presenta un modelo general de diseño para obtener el espesor y áreas de acero de refuerzo de zapatas rectangulares que soportan de 1 a "*n*" columnas alineadas sobre un eje longitudinal. El diagrama de presión se considera lineal. Algunos documentos publicados recientemente están restringidos a ciertos tipos de zapatas como zapatas rectangulares aisladas, y zapatas rectangulares combinadas que sostienen dos columnas. La primera parte de este artículo muestra el área mínima del suelo que soporta de 1 a "*n*" columnas alineadas en un eje longitudinal. Tres ejemplos numéricos se presentan para el diseño de zapatas rectangulares sometidas a una carga axial y dos momentos ortogonales en cada columna que soporta una, dos y tres columnas. La principal ventaja de este documento sobre otros documentos es: este modelo se puede aplicar para una o más columnas apoyadas en una zapata rectangular (sin restricciones en sus lados, un lado restringido y dos lados opuestos restringidos).

Palabras clave: modelo general para zapatas rectangulares; modelado para diseño; zapatas aisladas rectangulares; zapatas combinadas rectangulares.

1 Introduction

Fig. 1 shows the distribution of the soil pressure below of the footing, and the distribution of the soil pressure is defined by the type and relative rigidity of the soil, the rigidity of the footing, and the depth of foundation at level of contact between the footing and the soil. Fig. 1(a) presents a concrete rigid footing resting in granular soil (sand or gravel). Fig. 1(b) shows a concrete rigid footing resting on a clay cohesive soil [1]. Now, to simplify the calculation, the hypothesis has been assumed that the soil is constituted by a bed of independent linear springs in such a way that the stresses that occur in the soil will be proportional to the displacements suffered by the foundation (the area of the real distribution is equal to the area of the uniform distribution).

How to cite: Rivera-Mendoza, J.B., Arnulfo Luévanos-Rojas, A., López-Chavarría, S., Medina-Elizondo, M. and García-Galván, M. A general model for rectangular footings part II: modeling for design. DYNA, 89(223), pp. 9-18, July - September, 2022.

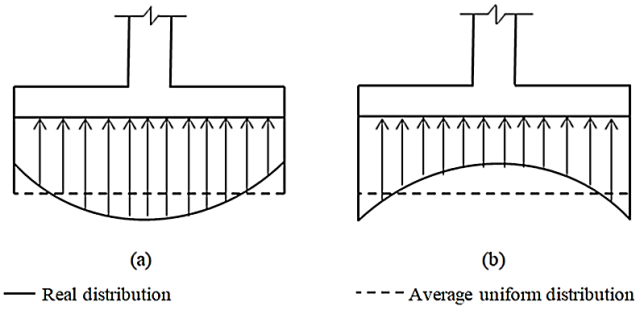

Figure 1. Distribution of the soil pressure below of the footing: (a) Rigid footing in non-cohesive soil (sand or gravel); (b) Rigid footing in clay cohesive soil.
Source: Prepared by the author.

The traditional design of footings generally involves a method of successive approximations. This process assumes a uniform distribution of stresses under the foundation, which represents an inadequate approach.

This work proposes direct equations to determine the effective depth and reinforcing steel areas of rectangular footings with different edge conditions for the calculation of bending moments, bending shear and punching shear for a linear distribution of stresses.

The works on mathematical models for foundation structures have been investigated successfully in several structural and geotechnical engineering problems. The main scientific contributions of several researchers in recent years are: Guler and Celep [2] presented the rectangular-shaped plate-column system by means of the Winkler foundation without tension under static and dynamic loads. Chen et al. [3] studied the hybrid composite plates on elastic foundations under nonlinear vibration. Smith-Pardo [4] presented a framework that considers the soil-structure interaction through simplified rocking foundation models. Shahin and Cheung [5] investigated the stochastic design charts for bearing capacity of strip footings. Zhang et al. [6] developed a nonlinear analysis of a finite beam resting on a Winkler foundation that takes into account the effect of the resistance of the beam on the soil. Agrawal and Hora [7] proposed the nonlinear interaction of a frame-footings-soil system under seismic loading. Rad [8] studied the static behavior of 2-D functionally graded circular plate with gradient thickness and elastic foundations for compound loads. Orbanich et al. [9] estimated the reinforcement and the repair with fiber composite materials for concrete foundation beams. Mohamed et al. [10] presented the Schmertmann general equation for settlement of shallow footings resting on saturated and unsaturated sands. Orbanich and Ortega [11] used the finite differences method for elastic foundation plates using internal and perimetric reinforcement beams rested on elastic foundations. Luévanos-Rojas et al. [12] developed a novel model for the design of rectangular isolated footings. Aristizabal-Ochoa [13] presented the general conditions for the stability of thin cross section columns rested on an elastic foundation. Barreto-Maya et al. [14] compared the load capacity between the experiment load tests and the mathematical formulations for deep foundations. Luévanos-Rojas [15] developed a mathematical model for the design of circular isolated footings. Uncuoğlu [16] investigated the load capacity for square footings on sand layer overlying clay. Luévanos-Rojas [17] developed a novel model for the design of boundary trapezoidal combined footings. Camero [18] presented a novel finite element method for the design of grade industrial floor slabs and pavements applying edge loads. Luévanos-Rojas [19] developed a mathematical model for the design of boundary rectangular combined footings limited to two opposite sides. Mohebkhah [20] estimated the load capacity of stone masonry strip footings over a clay trench. López-Chavarría et al. [21] proposed a novel mathematical model for the design of square isolated footings that takes into account the eccentric load on the footing (general case). Anil et al. [22] presented an analysis for footings of different shapes supported on sandy soil by the finite element method and experimental tests. Luévanos-Rojas et al. [23] presented a comparative study for design of trapezoidal and rectangular boundary combined footings using new models. Luévanos-Rojas et al. [24] proposed a novel mathematical model of design for the T-shaped combined footings. Yáñez-Palafox et al. [25] developed a modeling for the design of the strap combined footings.

The paper related to this work is: the design of rectangular combined footings of boundary with two opposite sides restricted that support two columns [19]. Thus, the review of the literature clearly shows that there is no close relationship with the topic of mathematical model for the design of rectangular footings that support one or more columns aligned on a longitudinal axis that is presented in this paper.

The first part of this document shows the most economical contact area on the soil (optimal surface) for the rectangular footings that support one or more columns aligned on a longitudinal axis. This paper presents a general model for the design of rectangular footings that support one or more columns aligned on a longitudinal axis. The pressure diagram considered in this document is linear. The recently published papers are restricted for same types of rectangular footings such as the rectangular isolated footings and rectangular combined footings (one paper for a restricted side and it considers that the resultant force is located on the longitudinal axis, and another paper for the two opposite sides restricted). Also, three numerical examples are shown to obtain the design of rectangular footings subject to an axial load and two moments in orthogonal directions in each column. First example is for a rectangular footing that supports a column (rectangular isolated footing). Second example is for a rectangular footing that supports two columns (rectangular combined footing). Third example is for a rectangular footing that supports three columns (rectangular combined footing).

2 Formulation of the general model

Fig. 1 of the part I shows a rectangular footing that supports "*n*" columns aligned on a longitudinal axis (X axis), and each column provides an axial load and two orthogonal bending moments.

Fig. 2 of the part I presents the pressure diagram below the rectangular footing, and also the soil pressure in each corner on the footing.

Stress anywhere on the footing contact surface due to soil pressure is presented below.

The stress in the main direction (longitudinal axis) of the X axis is (part I):

$$\sigma(x,y) = \frac{R}{L_x L_y} + \frac{12M_{xT}y}{L_x {L_y}^3} + \frac{12M_{yT}x}{{L_x}^3 L_y} \quad (1)$$

where: R is the sum of all the axial forces, M_{xT} is the sum of all the bending moments around the X axis and M_{yT} is the sum of all the bending moments around the Y axis, x is the distance parallel to the X axis measured from the center of gravity to the point in study, y is the distance parallel to the Y axis measured from the center of gravity to the point in study, L_x is the distance in X direction of the footing, L_y is the distance in Y direction of the footing. R, M_{xT}, M_{yT}, are presented in eq. (9)-(11) of the part I.

The stress in the transverse direction (Y axis) to the main direction (X axis) for any column by the following equation is obtained:

$$\sigma_{P_n}(x_n, y_n) = \frac{P_n}{w_n L_y} + \frac{12M_{xn}y}{w_n {L_y}^3} + \frac{12\left(M_{yn} + P_n e_{xn}\right)x}{L_y {w_n}^3} \quad (2)$$

where: x_n and y_n are the stress coordinates of the column n, P_n is the axial load in the column n, M_{xn} is the bending moment around the X axis in the column n, M_{yn} is the bending moment around the Y axis in the column n, w_n is the width of the analysis surface for the column n in the main direction (X axis). The width of the analysis surface for the column located closest to the property line is $w_n = s + c_{2n-1} + d/2$ (If $s \geq d/2 \rightarrow s = d/2$, and if $s < d/2 \rightarrow s = s$), and for the columns located in the central part of the footing the width of the analysis surface is $w_n = c_{2n-1} + d$ (d is the effective deep, s is the distance from the face of the column to the free end of the footing). The eccentricity e_{xn} for the column located in the property line is $e_{xn} = w_n/2 - s - c_{2n-1}/2$, and for the columns located in the central part of the footing the eccentricity is $e_{xn} = 0$.

2.1 Moments

Fig. 2 shows the critical sections for the bending moments according to the code are [26]: For the axes parallel to the X axis are: a_1, a_2, a_3 … a_{n-1}, a_n. For the axes parallel to the Y axis are: b_1, b_2, b_3 … b_{n-1}, b_n, and d_1, d_2, d_3 … d_{n-1}, d_n.

2.1.1 Moment around the xn´–xn´ axis of 0 ≤ yn ≤ Ly/2

The shear force V_{yn} is obtained by the pressure volume of the surface formed by the $x_n' - x_n'$ axis with a width w_n and the free end (top side of the Fig. 2) of the footing:

$$V_{y_n} = -\int_{-\frac{w_n}{2}}^{\frac{w_n}{2}} \int_{y_n}^{\frac{L_y}{2}} \sigma_{P_n}(x_n, y_n) dy_n dx_n \quad (3)$$

$$V_{y_n} = \frac{6M_{xn}{y_n}^2}{{L_y}^3} + \frac{P_n y_n}{L_y} - \frac{P_n L_y + 3M_{xn}}{2L_y} \quad (4)$$

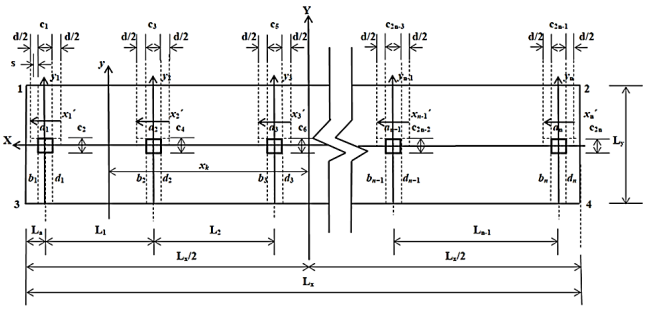

Figure 2. Critical sections of the bending moments.
Source: Prepared by the author.

Now, the integration of the shear force is the bending moment at any point, the basic equation is presented as follows:

$$V_{y_n} = \frac{dM_{x_n'}}{dy_n} \quad (5)$$

where: $M_{xn'}$ is the moment around the $x_{n'}$ axis and V_{yn} is the shear force at a distance y_n.

Integrating eq. (4) the bending moment at any point is obtained:

$$M_{x_n'} = \frac{2M_{xn}{y_n}^3}{{L_y}^3} + \frac{P_n{y_n}^2}{2L_y} - \frac{\left(P_n L_y + 3M_{xn}\right)y_n}{2L_y} + C_1 \quad (6)$$

Substituting $y_n = L_y/2$ and $M_{xn'} = 0$ into eq. (6), the constant C_1 is found:

$$C_1 = \frac{P_n L_y}{8} + \frac{M_{xn}}{2} \quad (7)$$

Now, substituting eq. (7) into eq. (6), the general equation for bending moments is shown as follows:

$$M_{x_n'} = \frac{P_n\left(2y_n - L_y\right)^2}{8L_y} + \frac{M_{xn}\left(4{y_n}^3 - 3{L_y}^2 y_n + {L_y}^3\right)}{2{L_y}^3} \quad (8)$$

Substituting $y_n = c_{2n}/2$ into eq. (8), the moment M_{an} on the a_n axis is obtained:

$$M_{a_n} = \frac{\left[P_n{L_y}^2 + 2M_{xn}\left(2L_y + c_{2n}\right)\right]\left(L_y - c_{2n}\right)^2}{8{L_y}^3} \quad (9)$$

2.1.2 Moment around the y–y axis considered the left part of the footing

The shear force V_{xk} is found by the pressure volume of the surface formed by the y - y axis with a width L_y and the free end (left side of the Fig. 2) of the footing:

$$V_{x_k} = \sum_{i=1}^{n} P_i - \int_{x_k}^{\frac{L_x}{2}} \int_{-\frac{L_y}{2}}^{\frac{L_y}{2}} \sigma(x,y) dy dx \quad (10)$$

$$V_{x_k} = \sum_{i=1}^{n} P_i - \left[\frac{R(L_x - 2x_k)}{2L_x} + \frac{3M_{yT}\left(L_x{}^2 - 4x_k{}^2\right)}{2L_x{}^3}\right] \quad (11)$$

where: the first part of eq. (10) and (11) represents the loads due to the columns and the second part represents the soil pressure.

Note: The shear forces due to column loads are not considered, when analyzed from the free end of the footing to the first column.

Now, the integration of the shear force is the bending moment at any point, the basic equation is presented as follows:

$$V_{x_k} = \frac{dM_y}{dx_k} \quad (12)$$

where: M_y is the moment around the y axis and V_{xk} is the shear force at a distance x_k.

Integrating the eq. (11) of the soil pressure and the bending moment at any point from the free end of the footing to the first column is obtained:

$$M_y = \frac{2M_{yT}x_k{}^3}{L_x{}^3} + \frac{Rx_k{}^2}{2L_x} - \frac{\left(RL_x + 3M_{yT}\right)x_k}{2L_x} + C_2 \quad (13)$$

Substituting $x_k = L_x/2$ and $M_y = 0$ into eq. (13) and the constant C_2 is obtained:

$$C_2 = \frac{RL_x}{8} + \frac{M_{yT}}{2} \quad (14)$$

Now, substituting eq. (14) into eq. (13), the general equation for bending moments at any point from the free end of the footing to the first column is shown as follows:

$$M_{y_1} = \frac{R(L_x - 2x_k)^2}{8L_x} + \frac{M_{yT}\left(L_x{}^3 - 3L_x{}^2x_k + 4x_k{}^3\right)}{2L_x{}^3} \quad (15)$$

Now, the eq. (11) of part I due to the columns loads are considered for the analysis from the column 1 until the last column. The bending moment at a distance "x_k" between the columns is:

$$M_{y_2} = -\sum_{i=1}^{n} M_{yi} - \sum_{i=1}^{n} P_i \left[\frac{L_x}{2} - L_a - \sum_{j=1}^{n=i-1} L_j - x_k\right] \quad (16)$$

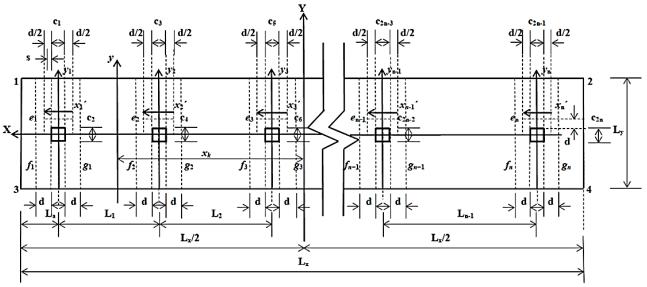

Figure 3. Critical sections of the bending shear.
Source: Prepared by the author.

where: M_{y1} is bending moment due to the soil pressure, and M_{y2} is bending moment due to column loads.

The eq. (15) and (16) are added to obtain the general equation of the bending moments at any point from the first column until the last column, and equation is represented as follow:

$$M_y = \frac{R(L_x - 2x_k)^2}{8L_x} + \frac{M_{yT}\left(L_x{}^3 - 3L_x{}^2x_k + 4x_k{}^3\right)}{2L_x{}^3} - \sum_{i=1}^{n} M_{yi} - \sum_{i=1}^{n} P_i \left[\frac{L_x}{2} - L_a - \sum_{j=1}^{n=i-1} L_j - x_k\right] \quad (17)$$

Substituting $x_k = L_x/2 - L_a + c_1/2$ into eq. (15), the bending moment M_{b1} on the b_1 axis is obtained:

$$M_{b_1} = \frac{\left[RL_x{}^2 + 2M_{yT}(3L_x - 2L_a + c_1)\right](2L_a - c_1)^2}{8L_x{}^3} \quad (18)$$

Now, substituting the coordinates in X direction at the junction of the column face with the footing to obtain the bending moments around of the axes b_2, b_3, … b_{n-1}, b_n, and d_1, d_2, d_3, … d_{n-1}, d_n.

2.2 Bending shear

Critical sections of the bending shear are presented at a distance d from the junction of the column with the footing, and these sections appear on en, fn and gn axes (see Fig. 3).

2.2.1 Bending shear on the $x_n' - x_n'$ axis

Substituting $y_n = c_{2n}/2 + d$ into eq. (4), the bending shear V_{en} on the e_n axis of the footing is obtained:

$$V_{e_n} = -\frac{3M_{xn}\left[L_y{}^2 - (c_{2n} + 2d)^2\right]}{2L_y{}^3} - \frac{P_n\left[L_y - (c_{2n} + 2d)\right]}{2L_y} \quad (19)$$

2.2.2 Bending shear on the y – y axis

Substituting $x_k = L_x/2 - L_a + c_1/2 + d$ into the second part of the eq. (11), the bending shear V_{f1} on the f_1 axis of the footing is obtained:

$$V_{f_1} = -\frac{3M_{yT}\left[L_x{}^2 - (L_x - 2L_a + c_1 + 2s)^2\right]}{2L_x{}^3} - \frac{R(2L_a - c_1 - 2s)}{2L_x} \quad (20)$$

where: the values of s are, if $s \geq d \rightarrow s = d$, and if s < d $\rightarrow s = s$.

Now, substituting the coordinates in X direction at a distance d from the junction of the column with the footing into eq. (11) to obtain the bending shear in the axes f_2, f_3, … f_{n-1}, f_n, and g_1, g_2, g_3, … g_{n-1}, g_n.

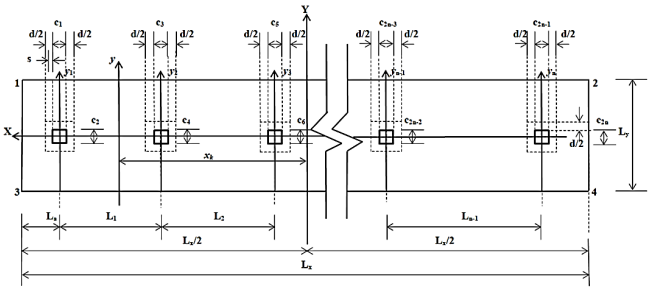

Figure 4. Critical sections of the punching shear.
Source: Prepared by the author.

2.3 Punching shear

Critical section for the punching shear appears at a distance *d/2* from the junction of the column with the footing in the two directions (see Fig. 4).

2.3.1 Punching shear for the boundary column

Critical section for the punching shear is presented in the rectangular section formed by the dotted surface of the boundary column. Punching shear acting on the footing V_{p1} is the force P_1 acting on column 1 subtracting the pressure volume of the surface formed by the dotted surface of the boundary column:

$$V_{p_1} = P_1 - \int_{\frac{L_x}{2}-L_a-\frac{(c_1+d)}{2}}^{\frac{L_x}{2}-L_a+\frac{(c_1+2s)}{2}} \int_{-\frac{(c_2+d)}{2}}^{\frac{(c_2+d)}{2}} \sigma(x,y)dydx \tag{21}$$

$$V_{p_1} = P_1 - \frac{R(2c_1+2s+d)(c_2+d)}{2L_xL_y} - \frac{\left[6M_{yT}\left(L_x-2L_a+s-\frac{d}{2}\right)\right]\left(c_1+s+\frac{d}{2}\right)(c_2+d)}{{L_x}^3L_y} \tag{22}$$

2.3.2 Punching shear for the inner column

Critical section for the punching shear is presented in the rectangular section formed by the dotted surface of the inner column. Punching shear acting on the footing V_{pn} is the force P_n acting on column *n* subtracting the pressure volume of the surface formed by the dotted surface of the inner column:

$$V_{p_n} = P_n - \int_{\frac{L_x}{2}-L_a-\sum_{j=1}^{n=i-1}L_j-\frac{(c_{2n-1}+d)}{2}}^{\frac{L_x}{2}-L_a-\sum_{j=1}^{n=i-1}L_j+\frac{(c_{2n-1}+d)}{2}} \int_{-\frac{(c_{2n}+d)}{2}}^{\frac{(c_{2n}+d)}{2}} \sigma(x,y)dydx \tag{23}$$

$$V_{p_n} = P_n - \frac{R(c_{2n}+d)(c_{2n-1}+d)}{L_xL_y} - \frac{6M_{yT}\left(L_x-2L_a-2\sum_{j=1}^{n=i-1}L_j\right)(c_{2n}+d)(c_{2n-1}+}{{L_x}^3L_y} \tag{24}$$

3 Numerical problems

Three numerical examples are presented below: Example 1 is for a rectangular footing that supports a column. Example 2 is for a rectangular footing that supports two columns. Example 3 is for a rectangular footing that supports three columns.

The thickness for the three examples is determined as follows: First, a minimum thickness is proposed according to the code of 25 cm [26], and then the thickness is revised to meet with the following conditions: bending moments, bending shear, and punching shear.

3.1 Example 1

The design of a rectangular footing (rectangular isolated footing) that supports a square column with the following information are presented: the column is of 40x40 *cm*; H = 2.0 *m*; P_{D1} = 600 *kN*; P_{L1} = 300 *kN*; M_{Dx1} = 200 *kN-m*; M_{Lx1} = 100 *kN-m*; M_{Dy1} = 100 *kN-m*; M_{Ly1} = 50 *kN-m*; f'_c = 35 *MPa*; f_y = 420 *MPa*; q_a = 250 *kN/m²*; γ_{ppz} = 24 *kN/m³*; γ_{pps} = 15 *kN/m³*. Where: H is the depth of the footing, P_{D1} is the dead load, P_{L1} is the live load, M_{Dx1} is the moment around the X axis of the dead load, M_{Lx1} is the moment around the X axis of the live load, M_{Dy1} is the moment around the Y axis of the dead load, M_{Ly1} is the moment around the Y axis of the live load.

The load and moments that act on soil are: P_1 = 900 *kN*; M_{x1} = 300 *kN-m*; M_{y1} = 150 *kN-m*.

The thickness that meets the bending moments, bending shear, and punching shear is of 45 *cm*.

Substituting the values of σ_p = 215.95 *kN/m²*, P_1 = 900 *kN*, M_{x1} = 300 *kN-m*, M_{y1} = 150 *kN-m*, $L_a = L_x/2$ into eq. (15)-(23) of part I and using the MAPLE-15 software are obtained: S_{tmin} = 8.27 *m²*, L_x = 2.03 *m*, L_y = 4.07 *m*, σ_1 = 215.95 *kN/m²*, σ_2 = 108.86 *kN/m²*, σ_3 = 108.86 *kN/m²*, σ_4 = 1.77 *kN/m²*.

Now the practical dimensions of the rectangular footing that supports a square column are: L_x = 2.05 *m*, L_y = 4.10 *m*.

Substituting the values of L_x = 2.05 *m*, L_y = 4.10 *m* in the same MAPLE-15 software are obtained: S_{tmin} = 8.40 *m²*, L_x = 2.05 *m*, L_y = 4.10 *m*, σ_1 = 211.55 *kN/m²*, σ_2 = 107.08 *kN/m²*, σ_3 = 107.08 *kN/m²*, σ_4 = 2.61 *kN/m²*.

The load and the bending moments around of the X and Y axes (factored mechanical elements) are [26]: P_{u1} = 1200 *kN*; M_{ux1} = 400 *kN-m*; M_{uy1} = 200 *kN-m*.

3.2 Example 2

The design of a rectangular footing (rectangular combined footing) that supports two square columns with the following information are presented: the columns are of 40x40 *cm*; H = 2.0 *m*; L_1 = 6.00 *m*; P_{D1} = 600 *kN*; P_{L1} = 300 *kN*; M_{Dx1} = 200 *kN-m*; M_{Lx1} = 100 *kN-m*; M_{Dy1} = 100 *kN-m*; M_{Ly1} = 50 *kN-m*; P_{D2} = 1200 *kN*; P_{L2} = 600 *kN*; M_{Dx2} = 400 *kN-m*; M_{Lx2} = 200 *kN-m*; M_{Dy2} = 200 *kN-m*; M_{Ly2} = 100 *kN-m*; f'_c = 35 *MPa*; f_y = 420 *MPa*; q_a = 250 *kN/m²*; γ_{ppz} = 24 *kN/m³*; γ_{pps} = 15 *kN/m³*.

The loads and moments that act on soil are: P_1 = 900 *kN*; M_{x1} = 300 *kN-m*; M_{y1} = 150 *kN-m*; P_2 = 1800 *kN*; M_{x2} = 600 *kN-m*; M_{y2} = 300 *kN-m*.

The thickness that meets the bending moments, bending shear, and punching shear is of 80 cm.

Substituting the values of σ_p = 212.80 *kN/m²*, P_1 = 900 *kN*, M_{x1} = 300 *kN-m*, M_{y1} = 150 *kN-m*, P_2 = 1800 *kN*, M_{x2} = 600 *kN-m*, M_{y2} = 300 *kN-m* into eq. (15)-(23) of part I and using the MAPLE-15 software are obtained: S_{tmin} = 21.99 *m²*, L_a = 0.20 *m*, L_x = 8.07 *m*, L_y = 2.73 *m*, M_{xT} = 900.00 *kN-m*, M_{yT} = 0.00 *kN-m*, R = 2700 *kN*, σ_1 = 212.80 *kN/m²*, σ_2 = 212.80 *kN/m²*, σ_3 = 32.71 *kN/m²*, σ_4 = 32.71 *kN/m²*.

Now the practical dimensions of the rectangular footing that supports two square columns are: L_x = 8.10 *m*, L_y = 2.75 *m*.

Substituting the values of L_x = 8.10 *m*, L_y = 2.75 *m* in the same MAPLE-15 software are obtained: S_{tmin} = 22.27 *m²*, L_a = 0.22 *m*, L_x = 8.10 *m*, L_y = 2.75 *m*, M_{xT} = 900.00 *kN-m*, M_{yT} = 1.00 *kN-m*, R = 2700 *kN*, σ_1 = 209.40 *kN/m²*, σ_2 = 209.33 *kN/m²*, σ_3 = 33.09 *kN/m²*, σ_4 = 33.02 *kN/m²*.

The loads and the bending moments around of the X and Y axes (factored mechanical elements) are [26]: P_{u1} = 1200 *kN*; M_{ux1} = 400 *kN-m*; M_{uy1} = 200 *kN-m*, P_{u2} = 2400 *kN*; M_{ux2} = 800 *kN-m*; M_{uy2} = 400 *kN-m*.

The factored resultant loads and the factored resultant bending moments by Eqs. (16) to (18) of part I are obtained: R_u = 3600 *kN*, M_{uxT} = 1200 *kN-m*, M_{uyT} = 60 *kN-m*.

3.3 Example 3

The design of a rectangular footing (rectangular combined footing) that supports three square columns with the following information are presented: the columns are of 40x40 *cm*; H = 2.0 *m*; L_1 = 6.00 *m*; P_{D1} = 600 *kN*; P_{L1} = 300 *kN*; M_{Dx1} = 200 *kN-m*; M_{Lx1} = 100 *kN-m*; M_{Dy1} = 100 *kN-m*; M_{Ly1} = 50 *kN-m*; P_{D2} = 1200 *kN*; P_{L2} = 600 *kN*; M_{Dx2} = 400 *kN-m*; M_{Lx2} = 200 *kN-m*; M_{Dy2} = 200 *kN-m*; M_{Ly2} = 100 *kN-m*; P_{D3} = 1200 *kN*; P_{L3} = 600 *kN*; M_{Dx3} = 400 *kN-m*; M_{Lx3} = 200 *kN-m*; M_{Dy3} = 200 *kN-m*; M_{Ly3} = 100 *kN-m*; f'_c = 35 *MPa*; f_y = 420 *MPa*; q_a = 250 *kN/m²*; γ_{ppz} = 24 *kN/m³*; γ_{pps} = 15 *kN/m³*.

The loads and moments that act on soil are: P_1 = 900 *kN*; M_{x1} = 300 *kN-m*; M_{y1} = 150 *kN-m*; P_2 = 1800 *kN*; M_{x2} = 600 *kN-m*; M_{y2} = 300 *kN-m*; P_3 = 1800 *kN*; M_{x3} = 600 *kN-m*; M_{y3} = 300 *kN-m*.

The thickness that meets the bending moments, bending shear, and punching shear is of 80 cm.

Substituting the values of σ_p = 212.80 *kN/m²*, P_1 = 900 *kN*, M_{x1} = 300 *kN-m*, M_{y1} = 150 *kN-m*, P_2 = 1800 *kN*, M_{x2} = 600 *kN-m*, M_{y2} = 300 *kN-m*, P_3 = 1800 *kN*, M_{x3} = 600 *kN-m*, M_{y3} = 300 *kN-m* into eq. (15)-(23) of part I and using the MAPLE-15 software are obtained: S_{tmin} = 37.47 *m²*, L_a = 0.20 *m*, L_x = 14.47 *m*, L_y = 2.59 *m*, M_{xT} = 1500.00 *kN-m*, M_{yT} = 0.00 *kN-m*, R = 4500 *kN*, σ_1 = 212.80 *kN/m²*, σ_2 = 212.80 *kN/m²*, σ_3 = 27.37 *kN/m²*, σ_4 = 27.37 *kN/m²*.

Now the practical dimensions of the rectangular footing that supports two square columns are: L_x = 14.50 *m*, L_y = 2.60 *m*.

Substituting the values of L_x = 14.50 *m*, L_y = 2.60 *m* in the same MAPLE-15 software are obtained: S_{tmin} = 37.70 *m²*, L_a = 0.22 *m*, L_x = 14.50 *m*, L_y = 2.60 *m*, M_{xT} = 1500.00 *kN-m*, M_{yT} = 1.00 *kN-m*, R = 4500 *kN*, σ_1 = 211.19 *kN/m²*, σ_2 = 211.17 *kN/m²*, σ_3 = 27.56 *kN/m²*, σ_4 = 27.53 *kN/m²*.

The loads and the bending moments around of the X and Y axes (factored mechanical elements) are [26]: P_{u1} = 1200 *kN*; M_{ux1} = 400 *kN-m*; M_{uy1} = 200 *kN-m*, P_{u2} = 2400 *kN*; M_{ux2} = 800 *kN-m*; M_{uy2} = 400 *kN-m*, P_{u3} = 2400 *kN*; M_{ux3} = 800 *kN-m*; M_{uy3} = 400 *kN-m*.

The factored resultant loads and the factored resultant bending moments by Eqs. (16) to (18) of part I are obtained: R_u = 6000 *kN*, M_{uxT} = 2000 *kN-m*, M_{uyT} = − 1100 *kN-m*.

4 Results

One way to verify the model proposed in this document is:

Substituting $y_n = L_y/2$ into eq. (8), and the moment around the x_n'–x_n' axis is $M_{xn'} = 0$.

Now, substituting $x_k = L_x/2$ into eq. (15), and the moment around the y_1–y_1 axis is $M_{y1} = 0$.

Substituting $x_k = -L_x/2$ into eq. (17) and the moment around the y–y axis is $M_y = 0$.

Now, substituting $y_n = L_y/2$ into eq. (4) and the shear force on the x_n'–x_n' axis is $V_{yn} = 0$.

Substituting $x_k = L_x/2$ into eq. (11) considering only the second part that represents the soil pressure, and the shear force on the y_1–y_1 axis is $V_{xk} = 0$.

Now, substituting $x_k = -L_x/2$ into eq. (11), and the shear force on the y–y axis is $V_{xk} = 0$.

Therefore the equations for the bending moments and the shear forces are verified by equilibrium.

4.1 Example 1

Substituting the corresponding values into eq. (9)-(15) to obtain the bending moments that act on the critical sections of the rectangular isolated footing are shown below: M_{a1} = 671.68 *kN-m*; M_{b1} = 270.31 *kN-m*.

After making different proposals, the effective depth is d = 37.00 *cm*, r = 8.00 *cm*, t = 45.00 *cm*.

Substituting the corresponding values into eq. (19)-(20) to obtain the bending shear forces that act on the critical sections of the rectangular isolated footing are shown below: V_{e1} = − 568.20 *kN*; V_{f1} = − 367.43 *kN*. Now, the allowable bending shear forces by the concrete are: $\emptyset_v V_{ce1}$ = 648.42 *kN*; $\emptyset_v V_{cf1}$ = 1296.84 *kN*. Then, the two bending shear forces satisfy with the code [26].

Now, substituting the corresponding values into eq. (22) to obtain the punching shear force that acts on the critical section of the rectangular isolated footing is shown below: V_{p1} = 1115.35 *kN*. Now, the allowable punching shear forces by the concrete are: $\emptyset_v V_{cp1}$ = 2922.64 *kN*, $\emptyset_v V_{cp1}$ = 3236.86 *kN*, $\emptyset_v V_{cp1}$ = 1891.12 *kN*. Then, the punching shear force satisfies with the code [26].

The reinforcement steel areas for the rectangular isolated footing that result of the bending moments are shown below: A_{sy} = 50.39 *cm²*; A_{sx} = 19.50 *cm²*, and the minimum steel areas according to the code are [26]: A_{symin} = 25.28 *cm²*; A_{sxmin} = 50.57 *cm²*. Hence, the reinforcement steel areas for the design of the rectangular isolated footing are: A_{sy} = 50.39 *cm²*; A_{sx} = 50.57 *cm²*. The proposed steel areas are: A_{sy} = 50.70 *cm²* (10Ø1") spaced at 20.56 *cm*; A_{sx} = 50.70 *cm²* (10Ø1") spaced at 43.33 *cm*.

Table 1.
Bending shear forces of the example 2.

Axis	Shear force that acts (kN)	Allowable shear force (kN)	Width of analysis (m)
e_1	−319.05	467.79	0.76
e_2	−638.10	689.37	1.12
f_1	0*	1692.65	2.75
g_1	687.96	1692.65	2.75
f_2	−1165.61	1692.65	2.75
g_2	422.02	1692.65	2.75

* The axis falls outside of the footing
Source: Prepared by the author.

Table 2.
Punching shear forces of the example 2.

Analysis section	Shear force that acts (kN)	Allowable shear force (kN)	Critical perimeter (m)
Column 1 (boundary column)	1057.24	4948.69 8101.84 3202.09	2.68
Column 2 (inner column)	2198.61	8272.44 11347.38 5352.76	4.48

Source: Prepared by the author.

4.2 Example 2

Substituting the corresponding values into eq. (9), (15) and (17) to obtain the bending moments that act on the critical sections of the rectangular combined footing are shown below: $M_{a1} = 457.908$ *kN-m*; $M_{a2} = 915.80$ *kN-m*; $M_{b1} = 0.09$ *kN-m*; $M_{d1} = -400.33$ *kN-m*; $M_{b2} = 943.58$ *kN-m*; $M_{d2} = 692.53$ *kN-m*; $M_{max12} = -1540.55$ *kN-m* (maximum bending moment between the column 1 and column 2) in $x_{max12} = 1.37$ *m* (position of the maximum bending moment between the column 1 and column 2).

The maximum bending moment between the column 1 and column 2 is obtained as follows: First, the position of the maximum bending moment is located from the equation of the shear forces, i.e., when the shear force is zero, the maximum moment is obtained.

After making different proposals, the effective depth is $d = 72.00$ *cm*, $r = 8.00$ *cm*, $t = 80.00$ *cm*.

The bending shear forces that act on the critical sections of the rectangular combined footing by eq. (19)-(11), and the allowable bending shear forces for the concrete by the code are obtained [26] (see Table 1).

Then, the bending shear forces satisfy with the ACI code [26].

The punching shear force that act on the critical sections of the rectangular combined footing by eq. (22) and (24), and the allowable punching shear forces for the concrete by the code are obtained [26] (see Table 2).

Then, the two punching shear forces satisfy with the ACI code [26].

The reinforcement steel areas for the rectangular combined footing that result of the bending moments are shown below (see Table 3).

Table 3.
Reinforcement steel of the example 2.

Direction of the steel	Steel location		Steel area (cm^2)
Y axis	Under column 1 (width of $c_1 + s + d/2$)	Main steel	17.21
		Minimum steel	18.24
		Proposed steel	20.28(4Ø1")
	Under column 2 (width of $c_3 + d$)	Main steel	34.70
		Minimum steel	26.88
		Proposed steel	35.49(7Ø1")
	Steel at the bottom (width of $L_x - c_1 - c_3 - s - 3d/2$)	Temperature steel	89.57
		Proposed steel	91.20(32Ø3/4")
	Steel at the top (width of L_x)	Temperature steel	116.64
		Proposed steel	116.85(41Ø3/4")
X axis	Steel at the Bottom (width of L_y)	Main steel	35.11
		Minimum steel	66.00
		Proposed steel	70.98(14Ø1")
	Steel at the Top (width of L_y)	Main steel	57.80
		Minimum steel	66.00
		Proposed steel	70.98(14Ø1")

Source: Prepared by the author.

4.3 Example 3

Substituting the corresponding values into eq. (9), (15) and (17) to obtain the bending moments that act on the critical sections of the rectangular combined footing are shown below: Ma1 = 433.44 kN-m; Ma2 = 866.88 kN-m; Ma3 = 866.88 kN-m; Mb1 = 0.08 kN-m; Md1 = − 406.22 kN-m; Mb2 = − 73.36 kN-m; Md2 = 448.43 kN-m; Mb3 = 198.02 kN-m; Md3 = − 123.47 kN-m; Mmax12 = − 1797.11 kN-m (maximum bending moment between the column 1 and column 2) in xmax12 = 4.17 m (position of the maximum bending moment between the column 1 and column 2); Mmax23 = − 1794.99 kN-m (maximum bending moment between the column 2 and column 3) in xmax23 = − 1.71 m (position of the maximum bending moment between the column 2 and column 3).

The maximum bending moment between the two columns is obtained as follows: First, the position of the maximum bending moment is located from the equation of the shear forces, i.e., when the shear force is zero, the maximum moment is obtained.

After making different proposals, the effective depth is $d = 72.00$ *cm*, $r = 8.00$ *cm*, $t = 80.00$ *cm*.

The bending shear forces that act on the critical sections of the rectangular combined footing by eq. (19), (20) and (11), and the allowable bending shear forces for the concrete by the code are obtained [26] (see Table 4).

Then, the bending shear forces satisfy with the code [26].

The punching shear forces acting on the critical section of the rectangular combined footing by eq. (22) and (24) are obtained, and the allowable punching shear forces for the concrete by the code are obtained [26] (see Table 5).

Table 4.
Bending shear forces of the example 3.

Axis	Shear force that acts (kN)	Allowable shear force (kN)	Width of analysis (m)
e_1	−290.58	467.79	0.76
e_2	−581.16	689.37	1.12
e_3	−581.16	689.37	1.12
f_1	0*	1600.32	2.60
g_1	768.99	1600.32	2.60
f_2	−879.44	1600.32	2.60
g_2	759.28	1600.32	2.60
f_3	−988.95	1600.32	2.60
g_3	601.45	1600.32	2.60

* The axis falls outside of the footing
Source: Prepared by the author.

Table 5.
Punching shear forces of the example 3.

Analysis section	Shear force that acts (kN)	Allowable shear force (kN)	Critical perimeter (m)
Column 1 (boundary column)	1070.95	4948.69 8101.84 3202.09	2.68
Column 2 (inner column)	2202.51	8272.44 11347.38 5352.76	4.48
Column 3 (inner column)	2189.98	8272.44 11347.38 5352.76	4.48

Source: Prepared by the author.

Table 6.
Reinforcement steel of the example 3.

Direction of the steel	Steel location	Steel area (cm^2)	
Y axis	Under column 1 (width of $c_1 + s + d/2$)	Main steel	16.27
		Minimum steel	18.24
		Proposed steel	20.28(4Ø1")
	Under column 2 (width of $c_3 + d$)	Main steel	32.79
		Minimum steel	26.88
		Proposed steel	35.49(7Ø1")
	Under column 3 (width of $c_5 + d$)	Main steel	32.79
		Minimum steel	26.88
		Proposed steel	35.49(7Ø1")
	Steel at the bottom (width of $L_x - c_1 - c_3 - c_5 - s - 5d/2$)	Temperature steel	165.60
		Proposed steel	168.15(59Ø3/4")
	Steel at the top (width of L_x)	Temperature steel	208.80
		Proposed steel	210.90(74Ø3/4")
X axis	Steel at the Bottom (width of L_y)	Main steel	16.58
		Minimum steel	62.40
		Proposed steel	65.91(13Ø1")
	Steel at the Top (width of L_y)	Main steel	67.76
		Minimum steel	62.40
		Proposed steel	70.98(14Ø1")

Source: Prepared by the author.

Then, the two punching shear forces satisfy with the ACI code [26].

The reinforcement steel areas for the rectangular combined footing that result of the bending moments are shown below (see Table 6).

5 Conclusions

The model presented in this paper applies only for design of the rectangular footings that support n columns aligned on a longitudinal axis, this model assumes that the footings should be rigid and the supporting soil layers elastic, which meet expression of the bidirectional bending, i.e., the pressure variation behaves linearly.

This paper concludes the following:

1. The thickness for the rectangular isolated footing is governed by the bending shear on the e_1 axis, and the thicknesses for the rectangular combined footings that support two and three columns are governed by the bending shear on the e_2 axes.
2. This document is not limited as those presented by other authors such as: "Design of isolated footings of rectangular form using a new model" by Luévanos-Rojas [12], this model considers only a column. "A new model for the design of rectangular combined footings of boundary with two opposite sides restricted" by Luévanos-Rojas [19], this model considers only two columns.
3. The proposed model is more suited to the real conditions with respect to the classical model, because the proposed model takes into account the linear soil pressure and the classical model considers a uniform pressure (maximum pressure) in all the contact surface, when the loads and moments act on the footing.
4. The proposed model for design of rectangular footings subjected to an axial load and two moments in orthogonal directions in each column can be used for the following considerations:
   a) Without restrictions on their sides
   b) One side restricted
   c) Two restricted opposite sides

The main advantage of this document over other documents is that this model can be applied to one (rectangular isolated footings), two or more columns that are supported by a rectangular footing, and it is also not restricted to that the resultant force must be located on a longitudinal axis.

The next investigations can be: 1) Modeling for the design of foundation slabs and/or rafts. 2) When another type of soil is presented under the footing, by example in 100% cohesive soils (clay soils) or in 100% granular soils (sandy soils), the pressure diagram is different (nonlinear) and should be treated as shown in Fig. 1.

References

[1] Bowles, J.E., Foundation analysis and design. McGraw-Hill, New York, 2001.
[2] Guler, K. and Celep, Z., Response of a rectangular plate-column system on a tensionless Winkler foundation subjected to static and

dynamic loads. Structural Engineering and Mechanics, 21(6), pp. 699-712, 2005. DOI: https://doi.org/10.12989/sem.2005.21.6.699
[3] Chen, W-R., Chen, C-S. and Yu, S-Y., Nonlinear vibration of hybrid composite plates on elastic foundations. Structural Engineering and Mechanics, 37(4), pp. 367-383, 2011. DOI: https://doi.org/10.12989/sem.2011.37.4.367
[4] Smith-Pardo, J.P., Performance-based framework for soil-structure systems using simplified rocking foundation models. Structural Engineering and Mechanics, 40(6), pp. 763-782, 2011. DOI: https://doi.org/10.12989/sem.2011.40.6.763
[5] Shahin, M.A. and Cheung, E.M., Stochastic design charts for bearing capacity of strip footings. Geomechanics and Engineering, 3(2), pp. 153-167, 2011. DOI: https://doi.org/10.12989/gae.2011.3.2.153
[6] Zhang, L., Zhao, M.H., Xiao, Y. and Ma, B.H., Nonlinear analysis of finite beam resting on Winkler with consideration of beam-soil interface resistance effect. Structural Engineering and Mechanics, 38(5), pp. 573-592, 2011. DOI: https://doi.org/10.12989/sem.2011.38.5.573
[7] Agrawal, R. and Hora, M.S., Nonlinear interaction behaviour of infilled frame-isolated footings-soil system subjected to seismic loading. Structural Engineering and Mechanics, 44(1), pp. 85-107, 2012. DOI: https://doi.org/10.12989/sem.2012.44.1.085
[8] Rad, A.B., Static response of 2-D functionally graded circular plate with gradient thickness and elastic foundations to compound loads. Structural Engineering and Mechanics, 44(2), pp. 139-161, 2012. DOI: https://doi.org/10.12989/sem.2012.44.2.139
[9] Orbanich, C.J., Dominguez, P.N. and Ortega, N.F., Strenghtening and repair of concrete foundation beams whit fiber composite materials. Materials and Structures, 45, pp. 1693-1704, 2012. DOI: https://doi.org/10.1617/s11527-012-9866-6
[10] Mohamed, F.M.O., Vanapalli, S.K. and Saatcioglu, M. Generalized Schmertmann equation for settlement estimation of shallow footings in saturated and unsaturated sands. Geomechanics and Engineering, 5(4), pp. 363-377, 2013. DOI: https://doi.org/10.12989/gae.2013.5.4.343
[11] Orbanich, C.J. and Ortega, N.F., Analysis of elastic foundation plates with internal and perimetric stiffening beams on elastic foundations by using Finite Differences Method. Structural Engineering and Mechanics, 45(2), pp. 169-182, 2013. DOI: https://doi.org/10.12989/sem.2013.45.2.169.
[12] Luévanos-Rojas, A., Faudoa-Herrera, J.G., Andrade-Vallejo, R.A. and Cano-Alvarez M.A., Design of isolated footings of rectangular form using a new model. International Journal of Innovative Computing, Information and Control, 9(10), pp. 4001-4022, 2013. DOI: http://www.ijicic.org/ijicic-12-10031.pdf
[13] Aristizabal-Ochoa, J.D., Stability of slender columns on an elastic foundation with generalised end conditions. Ingeniería e Investigación, 33(3), pp. 34-40, 2013.
[14] Barreto-Maya, A.P., Valencia-González, Y. y Echeverri-Ramírez, O., Evaluación comparativa de la capacidad de carga en cimentaciones profundas. Fórmulas analíticas y ensayos de carga. Boletín Ciencias de la Tierra, 33, pp. 93-110, 2013.
[15] Luévanos-Rojas, A., Design of isolated footings of circular form using a new model. Structural Engineering and Mechanics, 52(4), pp. 767-786, 2014. DOI: https://doi.org/10.12989/sem.2014.52.4.767
[16] Uncuoğlu, E., The bearing capacity of square footings on a sand layer overlying clay. Geomechanics and Engineering, 9(3), pp. 287-311, 2015. DOI: https://doi.org/10.12989/gae.2015.9.3.287
[17] Luévanos-Rojas, A., Design of boundary combined footings of trapezoidal form using a new model. Structural Engineering and Mechanics, 56(5), pp. 745-765, 2015. DOI: https://doi.org/10.12989/sem.2015.56.5.745
[18] Camero, H.E., A novel finite element method for designing floor slabs on grade and pavements with loads at edges. Ingeniería e Investigación, 35(2), pp. 15-22, 2015. DOI: https://doi.org/10.15446/ing.investig.v35n2.45603
[19] Luévanos-Rojas, A., A new model for the design of rectangular combined boundary footings with two restricted opposite sides. Revista ALCONPAT, 6(2), pp. 172-187, 2016. DOI: https://doi.org/10.21041/ra.v6i2.137
[20] Mohebkhah, A., Bearing capacity of strip footings on a stone masonry trench in clay. Geomechanics and Engineering, 13(2), pp. 255-267, 2017. DOI: https://doi.org/10.12989/gae.2017.13.2.255
[21] López-Chavarría, S., Luévanos-Rojas, A. and Medina-Elizondo, M., A new mathematical model for design of square isolated footings for general case. International Journal of Innovative Computing, Information and Control, 13(4), pp. 1149-1168, 2017. DOI: http://www.ijicic.org/ijicic-130406.pdf
[22] Anil, Ö, Akbaş, S.O., BabagĪray, S., Gel, A.C. and Durucan, C., Experimental and finite element analyses of footings of varying shapes on sand. Geomechanics and Engineering, 12(2), pp. 223-238, 2017. DOI: https://doi.org/10.12989/gae.2017.12.2.223
[23] Luévanos-Rojas, A., Barquero-Cabrero, J.D., López-Chavarría, S. and Medina-Elizondo, M., A comparative study for design of boundary combined footings of trapezoidal and rectangular forms using new models. Coupled Systems Mechanics, 6(4), pp. 417-437, 2017. DOI: https://doi.org/10.12989/csm.2017.6.4.417
[24] Luévanos-Rojas, A., López-Chavarría, S. and Medina-Elizondo, M., A new model for T-shaped combined footings. Part II: mathematical model for design. Geomechanics and Engineering, 14(1), pp. 61-69, 2018. DOI: https://doi.org/10.12989/gae.2018.14.1.061
[25] Yáñez-Palafox, J.A., Luévanos-Rojas, A., López-Chavarría, S. and Medina-Elizondo, M., Modeling for the strap combined footings. Part II: mathematical model for design. Steel Composite Structures, 30(2), pp. 109-121, 2019. DOI: https://doi.org/10.12989/scs.2019.30.2.109
[26] American Concrete Institute. Building Code requirements for structural concrete and commentary. Committee 318. New York, 2019.

J.B. Rivera-Mendoza, received a MSc. in Business Administration in 1985, and the PhD in Administration and Senior Management in 2018, all of thrm from the Facultad de Contaduría y Administración of the Universidad Autónoma de Coahuila, Torreón, Coahuila, Mexico. He is professor and researcher of the Universidad Autónoma de Coahuila (2018-Current). His research interests are mathematical models applied to Administration. He has 5 papers published in international scientific research Journals.
ORCID: 0000-0002-0514-0796

A. Luévanos-Rojas, received his BSc. Eng. in Civil Engineering in 1981, his MSc. in Planning and Construction in 1996, and the PhD Engineering in Planning and Construction in 2009, all of them from the Facultad de Ingeniería, Ciencias y Arquitectura of the Universidad Juárez del Estado de Durango, Gómez Palacio, Durango, México. He received the MSc. in Structures in 1983, from the Escuela Superior de Ingeniería y Arquitectura the Instituto Politécnico Nacional, Distrito Federal, México. Also, he received the MSc. in Administration in 2004, from the Facultad de Contaduría y Administración of the Universidad Autónoma de Coahuila, Torreón, Coahuila, Mexico. He is professor and researcher of the Universidad Autónoma de Coahuila (2015-Current). He has more than 100 papers published in international scientific research Journals. His research interests include: mathematical models applied to structures. He is a member of the National System of Researchers of Mexico.
ORCID: 0000-0002-0198-3614

S. López-Chavarría, received his BSc. in Public Accountant, his MSc. in Administration, and the PhD in Administration and Senior Management from the Facultad de Contaduría y Administración of the Universidad Autónoma de Coahuila, Torreón, Coahuila, Mexico. She is professor and researcher of the Universidad Autónoma de Coahuila (2000-Current). His research interests include mathematical models applied to structures, methods of structural analysis, design of concrete and steel structural members, and analysis of non-prismatic members. She has more than 50 papers published in national and international scientific research Journals. She has been a speaker at scientific meetings in España, Colombia, Argentina. She is a member of the National System of Researchers of Mexico.
ORCID: 0000-0001-8909-1794

M. Medina-Elizondo, received his BSc. in Public Accountant, his MSc. in Administration from the Facultad de Contaduría y Administración of the Universidad Autónoma de Coahuila, Torreón, Coahuila, Mexico. He received the PhD in Administration Sciences from the Universidad Nacional Autónoma de México, Distrito Federal, Mexico. Also, he received the PhD in Administration Sciences from the Universidad de Newport, U.S.A. He is professor and researcher of the Universidad Autónoma de Coahuila (1988-Current). His research interests include mathematical models applied to structures, methods of structural analysis, design of concrete and steel

structural members, and analysis of non-prismatic members. He has more than 80 papers published in national and international scientific research Journals.
ORCID: 0000-0002-6113-4964

M. García-Galván, received a MSc. in International Business Law in 2002, from the ITESM in Monterrey Campus, and the PhD in Administration and Senior Management in 2018, from the Facultad de Contaduría y Administración of the Universidad Autónoma de Coahuila, Torreón, Coahuila, Mexico. She is professor and researcher of the Universidad Autónoma de Coahuila (2018-Current). His research interests are mathematical models applied to Administration. She has 5 papers published in international scientific research Journals.
ORCID: 0000-0001-8854-0930